

## Empirical evidence for a two phase system in SiCN films prepared by low pressure PE-CVD

T. Kawabe<sup>1</sup>, R. Cormia<sup>2</sup>, T. Wydeven<sup>1</sup>, V. Crist<sup>3</sup> and Z. Tanaka<sup>4</sup>

<sup>1</sup>SAMCO Inc. Sunnyvale, CA, U.S.A.

<sup>2</sup>Foothill College, Los Altos Hills, CA, U.S.A.

<sup>3</sup>Nanolab Technologies, Inc., San Jose, CA, U.S.A.

<sup>4</sup>NASA-Ames, Mountain View, CA, U.S.A.

**Abstract:** Silicon carbon nitride films were deposited on silicon wafers at 1,000 °C by RF-PECVD from a gas mixture of silane, methane and nitrogen. The films were analyzed by high resolution XPS, Raman spectroscopy, spectroscopic ellipsometry, profilometry and micro-indentation for hardness and Young's modulus. The experimental results from this work provide support for the two phase model for silicon carbon nitride that was proposed by others (Liao et al., J Euro Ceram Soc. 2012;32:1275-1281).

**Keywords:** SiCN films, RF-PECVD, SiCN model

### 1. Introduction

A study was undertaken to expand on previous efforts to deposit silicon carbon nitride (SiCN) films using PE-CVD (Kawabe, Wydeven, 11<sup>th</sup> APCPST, Oct-2012, Kyoto, Japan), improve on hardness, film stress, and optical properties, and better understand the chemical bonding of silicon, carbon, and nitrogen in the deposited films. Building on the previous work, various mixtures of ½ % silane in nitrogen, and pure methane, were combined in a PE-CVD reactor at 1,000 °C, and physical properties measured for each condition. A combination of XPS (X-Ray Photoelectron Spectroscopy), Raman Spectroscopy, and FTIR (Fourier Transform Infrared Spectroscopy) was done to better understand the chemical bonding networks in the deposited SiCN films. Composition, chemical bonding, and structural assignments from XPS and Raman, and Si-N species abundance from FTIR, aided interpretation of physical properties data, and provided a foundation for speculating about the nature of carbon and silicon nitride networks in the thin films. An emphasis of this investigation was determining if the films

could comprise separate carbon and silicon nitride networks, as suggested by Liao et al.

### 2. Experimental

Shown in Figure 1 is a drawing of the deposition chamber used for depositing the SiCN films by 13.56 MHz RF-PECVD. The figure also shows an expanded view of the substrate holder and sample heater. Shown in Table 1 are the deposition conditions used for preparing SiCN films in the experiments.

Each film was analyzed by XPS using a Thermo K-Alpha XPS spectrometer at a depth of 200Å (20 nm ion etch). Raman spectroscopy was performed on films with 20% carbon concentration and higher using a Renishaw

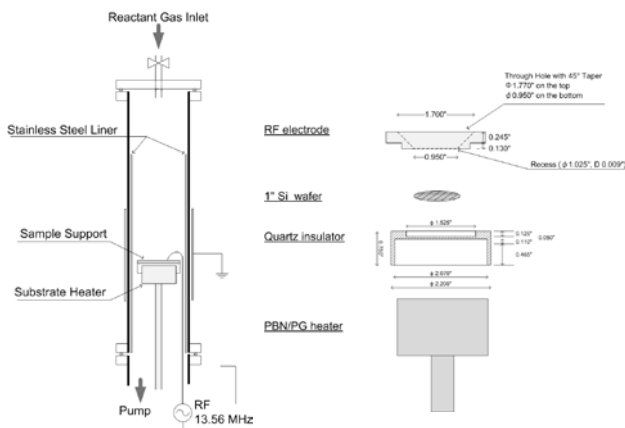


Fig.1 Deposition Chamber

Table 1. Deposition conditions used for preparing SiCN films on silicon substrates\* by PECVD

Gas composition:	variable**
Gas pressure, mTorr:	200
Total gas flow rate, SCCM:	50
RF power, Watts:	100
Substrate temperature, °C:	1000
Deposition time, minutes:	30

\*1 inch diameter silicon wafers (P type, B doped, 100 orientation, 250-350 µm thickness, 1-20 ohm-cm resistivity, polished side coated)

\*\*0.00-0.25 SCCM SiH<sub>4</sub>, 0.50-50.00 SCCM CH<sub>4</sub> and 0.00-49.25 SCCM N<sub>2</sub>

Table 2. Deposition rate, refractive index & film stress

Sample	Thickness, nm	Deposition Rate, nm/min	Refractive Index @632.8nm	Compressive stress, GPa
#325	500	16.7	2.23	1.5
#328	546	18.2	2.00	-
#329	552	18.3	1.97	1.0
#343	272	9.1	2.18	1.1
#346	294	9.8	1.98	1.4
#348	318	10.3	1.96	1.9

\*SR is unable to measure the thickness of films containing more than 60% of carbon because their light absorption is significant.

inVia Raman Microscope. FTIR was used to characterize three of the films, and hardness and optical measurements were performed on the selected films. All of the films were measured their thickness and refractive index by SR using a Filmetrics F20-UV. A CSM Instruments Nano Hardness Tester TTX-NHT with an indenter of Berkovich geometry was used to perform the indentation testing to measure the hardness and Young's modulus of the selected films. Shown in Table 2 are the deposition rate, refractive index, and film stress obtained by SR (Spectral Reflectance) and stylus surface profilometry and metrology.

### 3. Results and Discussions

#### XPS

Shown in Table 3 are the surface composition derived from XPS survey scans of the SiCN samples used to construct Figure 6. The survey scans were recorded after the as-prepared films were etched for 4-5 minutes using 500 eV Ar<sup>+</sup> to remove atmospheric contaminants such as oxygen and water vapor from the surface. Any oxygen detected after etching the as-prepared sample was probably derived from background oxygen present in the reac-

Table 3. Film composition from XPS, including N/Si elemental ratios

Sample	Gas Composition, %			Film Composition, %					N/Si Ratio
	SiH <sub>4</sub>	CH <sub>4</sub>	N <sub>2</sub>	C1s	O1s	N1s	Si2p	Ar2p	
#348	0.50	1.00	98.51	4.8	3.6	47.2	43.5	0.8	1.09
#346	0.49	2.00	97.51	9.2	4.7	44.9	40.5	0.8	1.11
#329	0.48	4.00	95.52	24.5	4.7	36.1	33.4	1.3	1.08
#328	0.46	8.00	91.54	33.1	4.5	31.9	29.1	1.3	1.10
#325	0.42	16.00	83.58	45.8	2.7	26.5	24.1	0.8	1.10
#343	0.38	24.00	75.62	51.6	2.8	20.6	24.0	1.0	0.86
#326	0.34	32.00	67.66	67.4	2.7	14.3	14.7	1.0	0.97
#338	0.28	44.00	55.72	81.4	2.0	8.1	7.1	1.5	1.14
#340	0.23	54.00	45.77	92.0	1.5	2.2	2.0	1.8	1.10
#332	0.18	64.00	35.82	93.2	1.0	2.1	2.0	1.8	1.05
#334	0.10	80.00	19.90	95.7	0.7	0.7	0.6	2.4	1.17
#336	0.20	96.00	3.98	95.9	0.7	0.4	0.5	2.5	0.80
#342	0.00	100.00	0.00	96.7	0.9	0.0	0.0	2.4	-

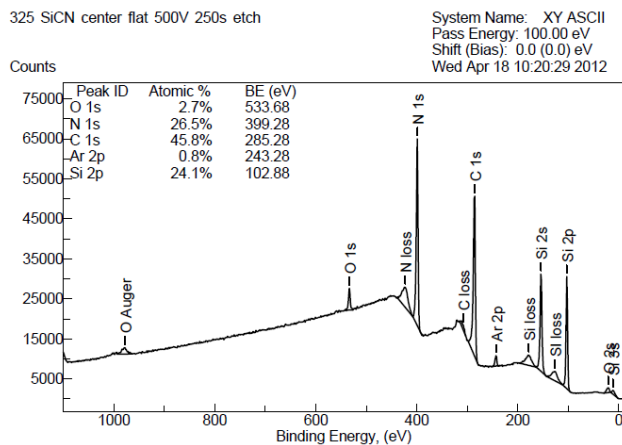


Fig. 2 Survey Spectrum of Representative SiCN sample

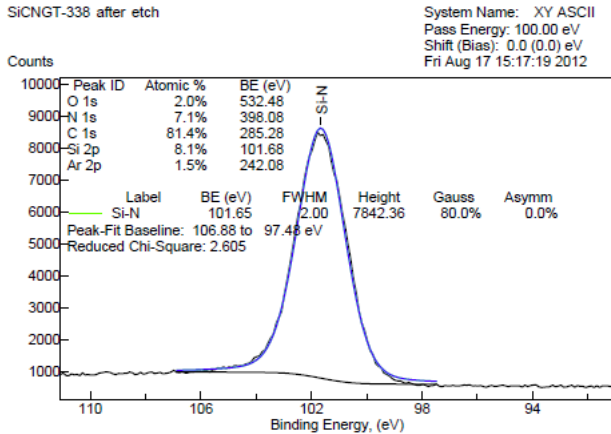
tor during deposition. Argon in the samples was derived from argon used to etch the samples.

Each film was argon ion etched to a depth of ~20 nm to remove surface oxidation and reach a uniform film composition before XPS analysis. Survey scan measurements from 0 – 1,100 eV were used to determine surface composition, and high resolution measurements of the Si(2p), C(1s), N(1s), and O(1s) spectral regions acquired to determine chemical bonding environments for those elements. A typical survey spectrum from the films is shown in figures 2, and high resolution data for Si(2p), C(1s), N(1s), and O(1s) are shown in figure 3. Curve fitting of the high resolution spectral data provided relative abundance and binding energies of chemical species assigned for each element. The composition and chemical bonding states from the XPS measurements are shown in tables 3. From these data a number of important trends were observed:

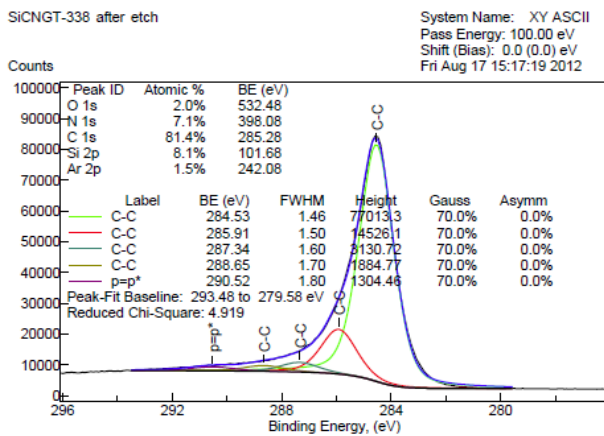
1. The composition of the films varied approximately with the gas mixtures of methane and silane, with N/Si ratios ranging from 0.8 to 1.2. The nitrogen to silicon ratio is nearly constant around its average of 1.05.
2. The abundance of carbon trends predictably with the square-root of methane flow rate (sccm), to nearly 80% carbon, as shown in figure 6.
3. Both N(1s) and Si(2p) spectral measurements show prominent peaks at ~398 eV and ~102 eV associated with silicon nitride, and the binding energy split between these two key peaks is nearly constant at 296 eV, with a slight trend from 296 to 297.5 eV as the concentration of carbon increases from 50 to 90% ( $r^2 \sim 80\%$ ).
4. The Si(2p) peak envelope is dominated by the Si<sub>x</sub>N<sub>y</sub> nitride peak at 102 eV, however a small peak at ~100 eV associated with silicon carbide appears at higher carbon abundance. This peak is assigned as the point where carbon is attached to silicon and/or the silicon nitride phase.
5. The carbon C(1s) peak envelope is similar to previous results from 1% silane (N<sub>2</sub>)/methane mixtures, showing peaks at about 283 eV (carbide), a prominent peak at 285 eV (C-C, C-H), and peaks at ~286-287 eV (NR<sub>3</sub>), and ~288 eV (NR<sub>4</sub>), that trend with the elemental abundance of carbon.
6. The N(1s) peak typically shows three peaks at ~398 eV, ~400 eV, and ~403 eV (when N/Si > 1), associated with silicon nitride, NR<sub>3</sub>, and NR<sub>4</sub> (R=C,H), with the relative abundance of NR<sub>3</sub>, and NR<sub>4</sub> peaks trending higher as the carbon abundance increases in the films. When the N/Si elemental ratio is > 1, a fourth peak N(1s) peak at ~100 eV associated with silicon carbide appears at higher carbon abundance. This peak is assigned as the point where carbon is attached to silicon and/or the silicon nitride phase.



SiCNGT-338 Silicon High Resolution Scan



SiCNGT-338 Carbon High Resolution Scan



SiCNGT-338 Nitrogen High Resolution Scan

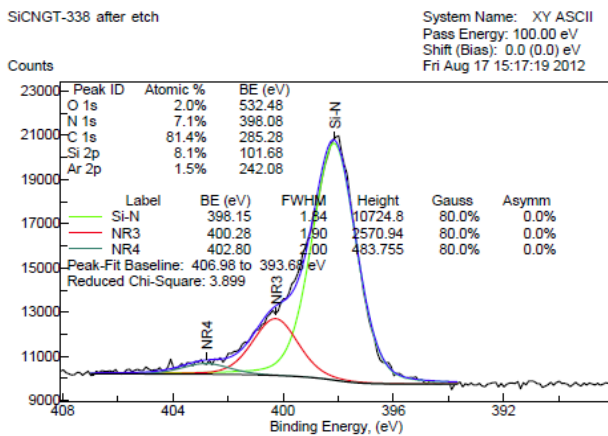


Fig.3 High resolution XPS scans for Si, C and N of a representative SiCN sample

7. In two films with very low abundances of carbon, 5 and 10 elemental %, the carbon peak envelope was dominated by strong carbide peaks at ~282 eV, with peaks at ~285 eV and ~287 eV associated with C-C and NR<sub>3</sub> peaks. The relative contribution of the carbide peak trended with decreasing carbon, and is a positive assignment for carbon bound directly to silicon.

8. In films with high concentrations of carbon (> 80%) that are also grayish in color, the C(1s) peak envelope and prominent binding energy (~284 eV) is more consistent with 'graphitic carbon'.

## Raman

Figure 4 shows three Raman spectra that were taken of SiCN films deposited at three different methane concentrations in the feed gas (samples #340, #342 and #343, Table 2). The spectra reveal a progressive increase in the structural order (as evidenced by a greater separation of the D and G bands in the spectra) in the films as the flow rate and carbon concentration increase. The sample prepared at the lowest methane flow rate is amorphous while that prepared at the highest methane flow rate mimics that of crystalline graphite. The key spectral features include the prominent D and G bands at ~1350 to 1375, and ~1580 to 1600 wave numbers, respectively, associated with the 'disorder' and 'ordered' sp<sup>2</sup> carbon networks. The 2D (G') region from ~ 2750 to ~3250 wave numbers, associated with the extended three dimensional (multi-layer networks) of graphene were also scanned. From these measurements, the following trends were observed in the films:

1. Films with 20 to 70% relative elemental abundance of carbon show D and G peaks that are not resolved, including broad and asymmetrical D peaks, and D/G ratios consistent with amorphous carbon. There was little if any peak structure between 2750 and 3250 wave numbers, consistent with amorphous carbon networks with little if any extended order (multilayer graphene).
2. At higher concentrations of carbon, above 70%, the D and G peaks become sharp and symmetrical, the D/G ratio decreases, and prominent 2D (G') peaks appear between 2750 and 3250 wave numbers, consistent with extended 3D order (multilayer

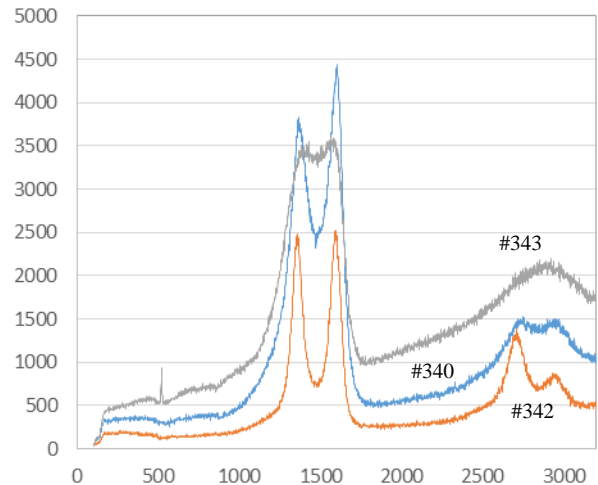


Fig.4 Raman spectrum of an amorphous SiCN sample (50 – 100 atomic% C)

graphene networks as observed in graphite).

- The Raman data suggest that, below 70%, % C follows square-root methane flow rate, and that the carbon is amorphous, lacking 3D order. In films above 70% carbon, and especially trending towards 90% carbon, the Raman data show clear evidence for graphitic carbon, and the degree of graphitic order trends with increasing carbon abundance.

### Methane and carbon correlation

By far one of the most striking results in this study was observation that the relative abundance of carbon in the films trends remarkably with the square-root of methane. Both XPS and Raman data also show consistent C(1s) peak envelopes, and nearly identical D/G peak structure, suggesting a consistent network structure for carbon, independent of silicon and nitrogen abundance. As mentioned earlier, the silicon Si(2p) and nitrogen N(1s) peak binding energies, peak splitting, and consistent N/Si abundance over the same five samples suggest that the silicon nitride network maintains a consistent structure as the carbon phase varies from 0 to 80%. The XPS and Raman data together are the strongest validation of the assertion by Liao et al. that amorphous SiCN PE-CVD films are independent two-phase networks. The square-root relationship for carbon deposition is not immediately understood, however it might be explained by a diffusion limited (Knudsen) process. One possible explanation of these results is the simultaneous deposition of carbon and silicon-nitride phases, but at different rates. XPS and Raman data are consistent with independent phases.

### Physical properties

The observed hardness of these films was not as high as desired, and limited to about 25 GPa as shown in Table 5. Refractive index varies from 1.96 to 2.23 as shown in Table 2.

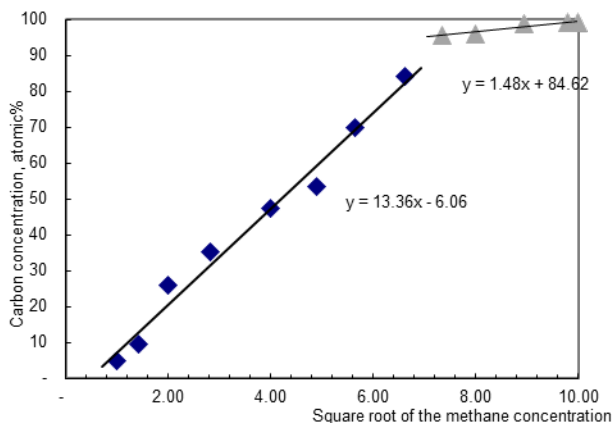


Figure 6. Atomic% C versus square root of methane concentration in the feed

Table 5. Microhardness and Young's Modulus of SiCN samples

Sample	Gas Composition, %			Hardness, GPa	Young's Modulus, GPa
	SiH <sub>4</sub>	CH <sub>4</sub>	N <sub>2</sub>		
#349	0.49	2.00	97.51	19.3	148.9
#350	0.49	2.00	97.51	20.4	145.4
#351	0.38	24.00	75.62	24.7	178.5
#352	0.38	24.00	75.62	21.5	183.6
#353	0.10	80.00	19.90	4.5	35.6
#354	0.10	80.00	19.90	5.1	35.0

### 4. Summary

- silicon carbon nitride films that ranged in composition from 10% to 90% carbon with nearly uniform N/Si ratios were successfully deposited on silicon wafer substrates at 1000 °C using RF-PECVD and a gas mixture of silane, methane and nitrogen
- the discovery that the N/Si ratio remained very near to 1 (1.05 +/- 0.10) while the carbon concentration in the SiCN films changed from 4.8 to 96.7 atomic% (see Table X) strongly suggests that the free-carbon & Si-N phases grow independently and their composition remains the same
- the rate of carbon deposition (inferred from the atomic% carbon) in SiCN films increased linearly with the square root of the methane concentration in the feed gas
- two ranges (range 1: methane flow rate from 0 to 25 SCCM and range 2: methane flow rate from 25 to 50 SCCM ) are apparent in which the kinetics of carbon deposition changes with methane concentration in the feed gas
- Raman spectra showed that the carbon phase in the SiCN films was amorphous except at high carbon concentrations, which showed C=C crystallinity suggestive of graphite
- the experimental results from this research are consistent with a 2-phase model for SiCN (Liao et al.); a free-carbon phase and a silicon nitride phase with the two phases chemically bonded by bridging bonds between Si-C and N-C